International Journal of Design & Nature and Ecodynamics
Vol. 21, No. 7, July, 2026, pp. 2031-2041
Journal homepage: http://iieta.org/journals/ijdne

Seismicity Clustering and Coulomb Stress Analysis of the Palu-Koro Fault

Harsano Jayadi[1,2], S. Sungkono[1*], Dwa Desa Warnana[3], Firman Syaifuddin[3], Gazali Rachman[4], Icha Untari Meidji[5], Iman Setiawan[6]

[1] Department of Physics, Institut Teknologi Sepuluh Nopember, Surabaya 60111, Indonesia
[2] Geophysical Engineering Study Program, Universitas Tadulako, Palu 94111, Indonesia
[3] Department of Geophysical Engineering, Institut Teknologi Sepuluh Nopember, Surabaya 60111, Indonesia
[4] Department of Physics Education, Universitas Pattimura, Maluku 97233, Indonesia
[5] Physics Study Program, Universitas Negeri Gorontalo, Bone Bolango 96583, Indonesia
[6] Statistics Study Program, Universitas Tadulako, Palu 94111, Indonesia

Corresponding Author Email: sungkono@its.ac.id

https://doi.org/10.18280/ijdne.210717

Received: 16 May 2026
Revised: 13 July 2026
Accepted: 22 July 2026
Available online: 31 July 2026

Keywords:
Palu-Koro Fault, Hierarchical Density-Based Spatial Clustering of Applications with Noise, Coulomb stress, seismic clustering, seismic hazard

ABSTRACT

This study examines seismic activity along the Palu-Koro Fault using the Hierarchical Density-Based Spatial Clustering of Applications with Noise (HDBSCAN) technique and Coulomb stress modeling based on earthquake data from 2011-2015. The findings reveal a highly diverse earthquake distribution, with stable seismic clusters corresponding to the geometry of the main fault. HDBSCAN can detect dense, high-density seismic cores and distinguish them from diffuse background seismicity without requiring a predetermined number of clusters. Coulomb stress modeling indicates that the most prominent clusters are spatially correlated with positive Coulomb Failure Stress ($\Delta CFS > 0$); this implies that static stress transfer from the 2012 mainshock was not the sole trigger for the localized earthquakes. The combined evaluation of clustering data and stress modeling reveals that structural segmentation and stress redistribution mechanisms control post-seismic seismic activity. This association yields a more physically constrained understanding of earthquake patterns than clustering or stress analysis alone. This approach combines data-driven seismic pattern recognition and geomechanical stress evolution to better identify fault segments with high seismicity potential.

1. INTRODUCTION

The Sulawesi region is one of the areas with the most complex tectonic conditions in Indonesia, as it lies within the interaction zone between the Eurasian/Sunda, Indo-Australian, and Philippine-Pacific plates [1-3]. This complexity has given rise to an actively developing fault system, including the Palu-Koro Fault. This fault, known as a left-lateral strike-slip fault, extends from the Palu Bay region to the southern part of Central Sulawesi and plays a crucial role in accommodating crustal deformation in Central Sulawesi. Information from geological and geodetic studies indicates that the Palu-Koro Fault has a relatively high slip rate of approximately 30-45 mm/year and therefore has the potential to trigger damaging earthquakes. However, some of its segments exhibit seismicity levels that do not always correspond to their deformation rates [4, 5]. This makes the Palu-Koro Fault one of the main natural laboratories for understanding the relationship between tectonic deformation, fault segmentation, and earthquake distribution in eastern Indonesia [4].

Activity along the Palu-Koro Fault has not only attracted attention following the major PASIGALA earthquake on 28 September 2018, but has also been documented through previous significant events. One such significant event was the earthquake on 18 August 2012, with a magnitude of approximately Mw 6.3, which occurred near the Palu-Koro Fault system. This earthquake had a predominantly lateral-slip mechanism and caused damage in the Palu, Sigi, and surrounding areas [6]. This event is important to study as it occurred before the 2018 earthquake and can provide insights into stress conditions, seismicity patterns, and the potential for active segmentation within the Palu-Koro Fault system. A study on the source mechanism of this earthquake indicates that the event is closely linked to strike-slip fault activity within the Palu-Koro system. Therefore, further analysis of the distribution of hypocentres and post-earthquake stress changes is crucial for understanding the local seismotectonic response [7].

Although the major PASIGALA earthquake of 2018 has been the primary focus of several seismotectonic studies in Central Sulawesi, it nevertheless retains scientific value, as it indicates the presence of moderate-to-strong seismic activity along the Palu-Koro Fault system before that earthquake. To reconstruct the seismicity patterns before, during, and after the 2012 earthquake, a critical analysis of earthquake data from the event period (2011-2015) is required. This is crucial for determining whether the earthquake is related to the activation of a specific segment, changes in stress distribution, or the migration of seismic activity along the fault zone. In this context, a relevant approach is the change in Coulomb Failure Stress (ΔCFS), as this can explain how earthquakes can alter shear stress and normal stress around the fault plane, causing certain areas to experience an increase in failure potential whilst others experience a decrease in stress, or 'shadow stress'. The relationship between faults and changes in Coulomb stress is crucial to understanding the patterns of seismic activity in the Palu-Koro Fault system and the surrounding structures. Studies on stress interactions and earthquake migration in Central Sulawesi demonstrate this in study [8]. Furthermore, Stein [9] emphasised that changes in static stress can correlate with changes in seismicity levels and the distribution of earthquakes, although the magnitude of this correlation is relatively small. Consequently, Coulomb stress analysis is used not only to determine whether clusters of earthquakes occur in areas experiencing increased stress, but also to determine the extent to which post-earthquake seismicity patterns are influenced by static stress transfer or other tectonic mechanisms operating along active fault systems.

In several previous studies, double-difference analysis has been used to link the distribution of the Palu-Koro earthquake on 18 August 2012 with changes in Coulomb stress [6, 8]. However, the correlations were inconsistent and suggested the presence of other contributing factors, such as fault geometry, subsurface heterogeneity, and uncertainty in hypocentre location. Hypocentre uncertainty and limitations in spatial estimation remain significant, as previous studies largely employed conventional linear methods. In this study, we employ NonLinLoc, which provides a three-dimensional probabilistic hypocentre estimate along with its uncertainty, thereby offering a stronger spatial foundation for analysing the distribution patterns of earthquakes and their relationship with changes in Coulomb stress [10-13]. In addition, the hypocentre results from NonLinLoc were analysed using Hierarchical Density-Based Spatial Clustering of Applications with Noise (HDBSCAN) clustering. This enables more accurate mapping of earthquakes and evaluation of the relationship between changes in Coulomb stress. This integrative method fills a gap in previous research and introduces innovation by combining probabilistic methods for hypocentre location with cluster analysis. This method also provides a much better understanding of seismic activation patterns and stress interactions within the Palu-Koro Fault system. The distribution of hypocentres is insufficient to objectively determine fault segmentation, as earthquake catalogues in active fault zones generally exhibit elongated, irregularly dispersed patterns and are spatially heterogeneous. Therefore, this study employs HDBSCAN as a complementary unsupervised clustering method.

Clustering approaches have been used to analyse earthquake catalogues and seismic data, thereby visualising seismicity patterns [14]. Density-based seismicity clustering to detect earthquake clusters and structural complexity in active tectonic and volcanic regions [15, 16]. Comparative studies have also investigated DBSCAN, HDBSCAN, and fuzzy clustering for seismic data in Indonesia [17]. This research reveals that clustering is an important and increasingly accepted strategy in contemporary seismological interpretation. However, this does not diminish the originality of this study, as the combined use of hypocentres obtained from NonLinLoc, HDBSCAN, and the Coulomb stress model has not yet been widely applied to the Mw 6.3 Palu-Koro earthquake sequence of 18 August 2012.

The uniqueness of this study lies in the development of an integrated seismic interpretation framework that explicitly integrates probabilistic hypocentre relocation, density-based adaptive clustering, and Coulomb stress modeling to identify the structural and mechanical factors influencing post-earthquake seismic activity. In contrast to previous studies that applied clustering methods to describe spatial patterns or used Coulomb stress analysis to infer potential triggers in isolation, this study demonstrates that earthquake clusters are physically meaningful only when validated against the stress redistribution field.

In the Palu-Koro Fault system, this integrated approach reveals that seismic activity patterns are governed by a dual-control mechanism: fault segmentation, which determines the geometry of spatial clustering, and static stress transfer, which governs the probability of activation for each cluster. Its main contribution is the identification of 'stress-consistent seismic nuclei', defined as high-density clusters derived from HDBSCAN [18, 19] that spatially coincide with positive ΔCFS anomalies. This enables statistical seismic structures to be interpreted directly in terms of mechanical failure potential, bridging the gap between data-driven clustering and geophysical stress modeling.

2. MATERIALS AND METHODS

2.1 Geological setting

The island of Sulawesi lies within a complex tectonic zone influenced by the interaction of several major plates and microblocks, including the Indo-Australian Plate, the Philippine-Pacific Plate, and the Sunda Block. This tectonic complexity has led to the formation of a network of active faults, subduction systems, microblock rotation, and significant crustal deformation. In West and Central Sulawesi, the Palu-Koro Fault is the main structure accommodating left-lateral deformation and serves as one of the primary boundaries between tectonic blocks [20].

The Palu-Koro Fault extends from a north-west to south-east direction to an almost north-south orientation, stretching from the offshore area of Palu Bay through Palu to the southern part of Central Sulawesi. The geometry of this fault is complex due to bends in its segments, branching structures, and its possible interconnection with surrounding fault systems. Previous studies on the 2018 Palu earthquake indicate that the fault zone can rupture across multiple segments, suggesting that segmentation is a key factor in determining earthquake hazard at this location [21].

Geological formations play a crucial role in earthquake studies in the Palu-Koro Fault region, which includes Quaternary alluvial deposits (Qa) [2, 22], metamorphic rock complexes (Tm) [23, 24], and Tertiary sedimentary rocks (Tmtv/Tmpb) [24, 25] (see Figure 1). The Quaternary alluvial deposits (Qa) in the Palu Basin consist of loose materials such as sand, gravel, and clay that are poorly consolidated; as a result, they can amplify seismic waves and increase liquefaction potential. The metamorphic rock complex (Tm) and Tertiary sedimentary rocks (Tmtv/Tmpb/Tmb) are the primary constituent rocks that have undergone deformation due to tectonic activity along the Palu-Koro Fault, thereby acting as zones for the accumulation and release of seismic energy [26, 27]. The combination of active faults and the characteristics of these rock formations makes this region highly vulnerable to earthquake hazards. These characteristics are important not only for earthquake hazard assessment, but also for the management of degraded land, spatial planning, and infrastructure development in regions with tectonic activity [28].

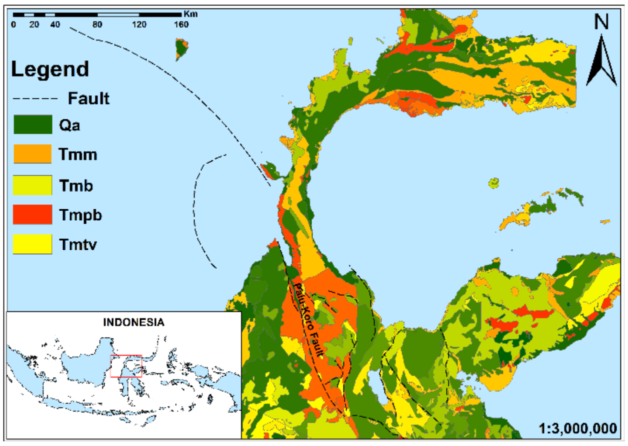

Figure 1. A geological map of Central Sulawesi and the surrounding area, showing various formations and minor faults around the Palu-Koro Fault
Note: Modified from research [29].

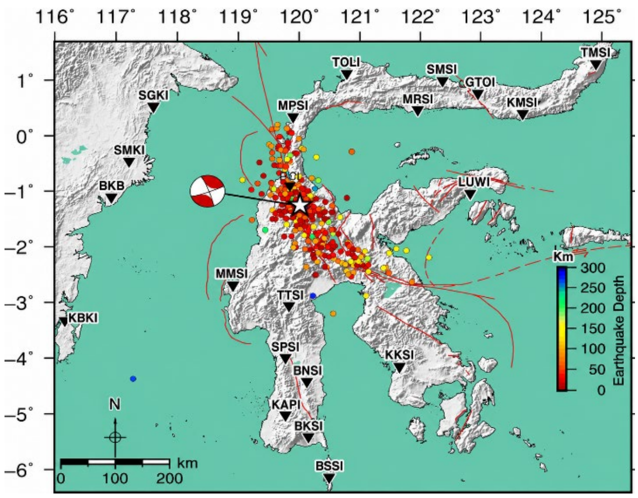

Figure 2. The distribution of earthquake events around the Palu-Koro Fault, both before and after the Mw 6.3 earthquake on 18 August 2012

2.2 Earthquake data

In this study, we used data from the local earthquake catalog of the BMKG network (http://geof.bmkg.go.id/webdc3/) covering the period from 1 January 2011 to 31 December 2015 in the Palu-Koro Fault and surrounding areas. The earthquake data comprised 398 events with magnitudes ≥ Mw 3, recorded by 21 BMKG stations (Figure 2). The selected timeframe covers the periods before, during, and after the Mw 6.3 earthquake on 18 August 2012, enabling this analysis to encompass both background seismicity and the post-mainshock aftershock sequence. The earthquake parameters included are time of occurrence, epicenter location, depth, magnitude, and arrival times of P- and S-waves, which were manually selected using NonLinLoc as the basis for analyzing the hypocenter distribution [10]. NonLinLoc was chosen because it employs a probabilistic, non-linear, and global search approach, enabling estimation of the hypocenter location and its spatial uncertainty, particularly in regions with complex velocity structures. The NLLoc program generates a misfit function that identifies the 'ideal' hypocenter by determining the probability density function (PDF). Utilize a PDF to ascertain the coordinates of the x, y, and z hypocentres employing one of the following methods: grid search systematic, stochastic Metropolis-Gibbs method, or oct-tree significance sampling techniques [11].

Meanwhile, the fault plane parameters (strike = 339°, dip = 82°, and rake angle = -5°) were obtained from the Global CMT catalog (https://www.globalcmt.org/) (Figure 2) to determine the length and width of the fault using calculations carried out for strike-slip faults [30]. This estimation process utilized the Coulomb 3.4 program [31, 32]. In this estimation, the input parameters used were Poisson's ratio (ν) = 0.25, Young's modulus (E) = 800,000 bar, and effective friction coefficient (μ′) = 0.4.

2.3 Hierarchical Density-Based Spatial Clustering of Applications with Noise clustering

The HDBSCAN clustering method is an extension of DBSCAN, utilizing a density-based, hierarchical algorithm. One of the advantages of this algorithm is its ability to handle clusters of various shapes, high dimensions, and an uncertain number of clusters; there is no need to specify an ideal number of clusters in advance, making this clustering method suitable for spatial data [18, 19, 33]. The main differences between HDBSCAN and DBSCAN lie in the distance function and the hierarchical structure, which is constructed based on the density between data points.

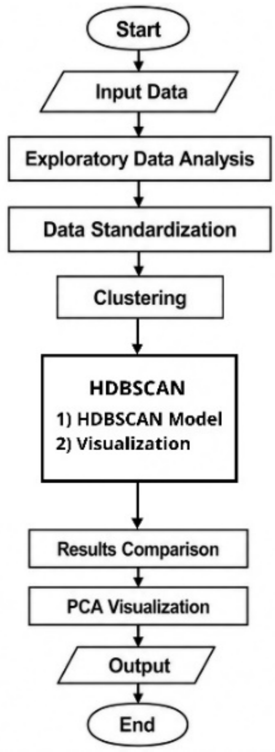

Figure 3. Flowchart model for earthquake data analysis using Hierarchical Density-Based Spatial Clustering of Applications with Noise (HDBSCAN) clustering

The flowchart (Figure 3) illustrates the workflow for earthquake clustering analysis using an unsupervised machine learning method, namely HDBSCAN clustering. The dataset contains three main variables: longitude, latitude, and earthquake depth. Initial exploration using the header (data) and summary (data) indicates that longitude values range from 117.3 to 122.1, latitude values range from -4.369 to 4.396, and earthquake depth values range from 1.089 km to 285.836 km, with an average depth of approximately 55.989 km.

Prior to clustering, longitude, latitude, and hypocentral depth were standardized using z-score normalization to remove differences in numerical scale. HDBSCAN was then applied to the standardized three-dimensional feature space using the default Euclidean distance metric implemented in the R dbscan package with minPts = 10. Following the original HDBSCAN algorithm, mutual reachability distances were first computed to account for local density differences, after which a minimum spanning tree (MST) was constructed. The hierarchical cluster tree was subsequently pruned based on cluster stability, and the most stable clusters were automatically extracted without requiring a predefined number of clusters.

We applied the HDBSCAN method directly to the standardized data with a minPts value of 10. HDBSCAN automatically determines the number of clusters and identifies observations that are noise or outliers. The analysis yielded four main clusters and one noise group (cluster 0). The resulting distribution comprises 195 observations classified as noise/outliers, whilst the remaining observations form clusters containing 15, 21, 16, and 151 earthquake events, respectively. The large number of noise points indicates that the earthquake distribution exhibits a heterogeneous, non-linear spatial pattern, which is common in seismic data from active fault systems with varying tectonic activity.

Following the clustering stage, the HDBSCAN method distinguishes dense seismic regions from rare events or anomalies. This feature makes HDBSCAN more flexible in identifying irregular seismic patterns and unusual earthquakes. Spatial visualizations are then generated using longitude and latitude coordinates to illustrate the distribution of the resulting earthquake clusters. Next, to further evaluate the cluster structure, we performed a principal component analysis (PCA) on the standardized dataset. PCA reduces multidimensional data using the first and second-highest Eigenvalues, allowing clustering patterns to be visualized in a lower-dimensional space. The resulting PCA plot from the HDBSCAN clustering was used to visualize cluster separation and data distribution patterns better. Consequently, the clustering results, including the cluster labels, were exported for further interpretation and seismic analysis.

2.4 Coulomb stress

In determining the source-fault inputs, we used several earthquake parameters, namely the epicentre coordinates, depth, magnitude, and strike, dip, and rake. Fault dimensions such as length (L), width (W), area (A), and displacement (D) were analysed using the empirical relationship [30] intended for thrust faults. Coulomb stress calculations were performed over a depth range of 0 to 30 km, at 5 km intervals. This depth range was selected based on the hypocenter of the main earthquake, located at approximately 13 km depth.

Assuming a simple Coulomb friction model for earthquakes, the potential slip will increase or decrease with ΔCFS [34], which is defined as Eq. (1):

$$\Delta CFS = \Delta\tau + \mu'\Delta\sigma_n \quad (1)$$

where ΔCFS is the Coulomb failure stress, $\Delta\tau$ denotes the shear stress, $\Delta\sigma_n$ indicates the sum of the normal stress and fluid pore pressure (P), and μ' is the effective friction coefficient. The normal stress is positive when the fault is unlocked and negative when it is locked, whilst the shear stress is positive for slip in the slip direction.

The value of P modifies the effective normal stress along the fault plane. When rock stress changes rapidly, P subsequently changes in a flow-like manner. The value of P can be related to Skempton's coefficient B, which varies between 0 and 1. The effective friction coefficient in coseismic stress studies ranges from 0.01 to 0.75, with an average of μ' = 0.4. ΔCFS is resolved on the first fault plane and in the direction of slip on the second fault plane or the receiver fault.

Where the effective stiffness is expressed as $\mu' = \mu(1 - \beta)$; furthermore, if ΔCFS > 0, the slip potential will increase, and if ΔCFS < 0, the slip potential will decrease. The calculation of ΔCFS caused by an earthquake depends on the geometry and distribution of slip, the assumed magnitude, the regional stress orientation, and the value of the assumed stiffness. The ratio of regional stress amplitude to earthquake stress drop has a significant impact only near the fault. In some cases, the uncertainty in ΔCFS is always dominated by that in the slip distribution. In principle, if ΔCFS > 0 (positive), it means that the first fault can cause the second fault to experience an increase in stress, making the likelihood of failure on the second fault greater. Conversely, if ΔCFS < 0 (negative), the first fault relaxes the second fault, thereby reducing the likelihood of failure; this region is often referred to as a stress shadow zone.

To strengthen the analytical framework, this study integrates deterministic geomechanical modelling and data-driven clustering techniques. Coulomb stresses were calculated using the Coulomb 3.4 software [31, 32], which is based on the theory of elastic dislocations in a homogeneous half-space. This model estimates the Coulomb Failure Stress (ΔCFS) as a function of the shear stress change ($\Delta\tau$), the normal stress change ($\Delta\sigma_n$), and the effect of pore-fluid pressure on an optimally oriented host fault. In this study, the Coulomb 3.4 software was applied to simulate the co-seismic stress disturbance associated with the Mw 6.3 Palu-Koro earthquake, using fault geometries derived from Global CMT solutions and empirical scaling relationships. Stress variations were evaluated at depth intervals of 0-30 km to capture vertical heterogeneity relevant to the hypocentre distribution. Positive ΔCFS values indicate stress loading and an increased potential for failure, whilst negative values represent stress-shadow zones that inhibit crack initiation. To identify spatial patterns, earthquake hypocentres were analysed using HDBSCAN [17, 18, 33] in R, with a minimum cluster size of 10. HDBSCAN identifies clusters of varying density without requiring a predefined number of clusters, making it suitable for irregular seismic distributions. This method distinguishes the dense core of earthquakes from background seismicity and noise. The combined use of Coulomb stress modelling and HDBSCAN clustering provides a highly complementary framework that links physical stress transfer with the structure of statistical seismicity.

The spatial correlation between the earthquake catalog and the ΔCFS grid was determined by superimposing the hypocenter coordinates onto the calculated Coulomb 3.4. For each earthquake, the relevant ΔCFS value was obtained from the grid node closest to the hypocenter, without using spatial interpolation. This methodology ensured that every seismic event was explicitly linked to a corresponding ΔCFS value derived from the calculated stress field for subsequent spatial and statistical analyses.

3. RESULTS

3.1 Hierarchical Density-Based Spatial Clustering of Applications with Noise clustering

The HDBSCAN results provide a more selective representation of areas with high seismicity. HDBSCAN only clusters points with strong density structures. Noise or background seismicity can be considered as points that do not meet a certain density threshold. As some earthquake events are concentrated in active fault zones, whilst others are scattered as isolated or low-density events, HDBSCAN is better suited to analysing earthquake catalogues, which typically have a non-homogeneous distribution.

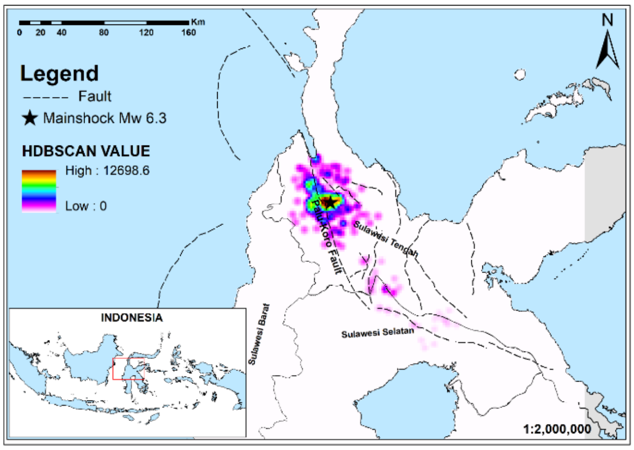

Figure 4. Distribution of seismicity density based on the HDBSCAN method

Note: Areas with high values indicate a high concentration of hypocentres around the epicentre of the Mw 6.3 earthquake and the main trend of the Palu-Koro Fault.

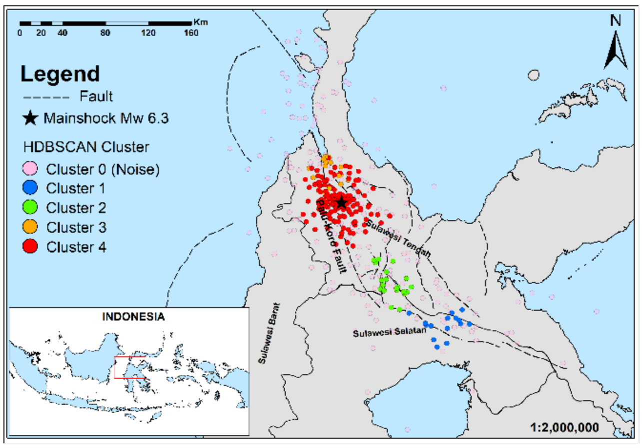

Figure 5. Distribution of seismicity clusters from the Mw 6.3 earthquake that occurred around the Palu-Koro Fault and its surroundings

On the HDBSCAN map, the highest-density locations are around the epicentre of the Mw 6.3 earthquake, which follows the Palu-Koro Fault (Figure 4). The zones with the most intense colour indicate locations with the highest concentration of seismic events. This region is situated around Palu and the central segment of the Palu-Koro Fault. A similar pattern is also evident in the HDBSCAN clustering results, which divide the locations of earthquake events in the study area into four clusters, plus the noise cluster (Figure 5).

An elongated pattern parallel to the fault structure is also clearly visible in the HDBSCAN distribution. This pattern is significant as it indicates that seismic activity follows the existing tectonic geometry, rather than forming a random cluster of points. Such elongated patterns may indicate zones of deformation influenced by lateral fault movement, as with the Palu-Koro Fault, which is classified as an active strike-slip fault. These results are consistent with seismotectonic studies in Central Sulawesi, which show that earthquake hypocentres tend to be located around the Palu-Koro system and adjacent fault structures. As demonstrated in this study [35], earthquake-induced displacement in the Palu region and its surroundings indicates a relationship between the distribution of hypocentres and active fault structures.

In the southeast and south, the HDBSCAN also reveals zones of moderate to low density. This pattern is significant as it may indicate a shift in activity towards other regions. This occurs despite lower concentrations near the epicentre. In an active fault system, stress changes caused by a single earthquake can increase the likelihood of earthquakes occurring in the surrounding areas. Therefore, zones of moderate density or small clusters should not be overlooked. The presence of these areas may indicate a secondary response to stress redistribution following an earthquake.

To evaluate the robustness of the clustering solution, a sensitivity analysis was conducted by varying the minPts parameter from 5 to 15. The overall spatial configuration of the four major seismic clusters remained largely unchanged for minPts values between 8 and 12, while only the number of observations classified as noise varied slightly. This result indicates that the identified seismic clusters are robust to moderate changes in parameter selection.

The ability of HDBSCAN can identify clusters with varying shapes and densities. According to studies [36, 37], HDBSCAN was developed from DBSCAN by incorporating a hierarchical structure and cluster extraction based on cluster stability, and is more robust to parameter variations than DBSCAN. This is because earthquake catalogues often contain complex spatial patterns; density-based approaches are increasingly used in contemporary seismological research to identify groups of earthquakes associated with seismotectonic processes and subsurface structures [16]. Consequently, the results of the HDBSCAN study are more consistent with the natural seismicity patterns around the Palu-Koro Fault.

Table 1. Cluster stability scores

Cluster	Stability
1	5.527
2	7.646
3	2.28
4	390.013

The HDBSCAN hierarchy produced positive stability scores for all four clusters (Table 1). Cluster 4 exhibited the highest stability score (390.013), indicating that it persisted over the widest range of density levels within the HDBSCAN hierarchy. The remaining clusters also showed positive stability values, confirming that they represent meaningful density-based seismic structures.

To evaluate the robustness of the HDBSCAN parameterization, a sensitivity analysis was performed using minPts values of 8, 10, and 12 (Table 2). All three parameter settings consistently identified four major seismic clusters, indicating that the overall clustering structure is robust to moderate variations in the minPts parameter. Only slight differences were observed in the number of events classified as noise (199, 195, and 204 events, respectively), suggesting that parameter changes primarily affected sparsely distributed earthquakes rather than the core seismic clusters. These results support the selection of minPts = 10 as a robust parameter for the final clustering analysis.

Table 2. Parameter sensitivity analysis

minPts	Clusters	Noise
8	4	199
10	4	195
12	4	204

3.2 Coulomb stress clustering

Zones with positive Coulomb stress appear to dominate around the epicentre of the Mw 6.3 earthquake in 2012 (Figure 6), extending in a direction that correlates with the geometry of the Palu-Koro Fault. According to Coulomb stress failure theory, an increase in positive stress (red-yellow) along a fault plane can increase the likelihood of earthquakes, particularly if the plane is orientated parallel to the induced stress. Conversely, regions experiencing a decrease in stress are characterised by zones of negative Coulomb stress (blue). As the rock system moves away from failure conditions in these regions, the likelihood of seismic activity may decrease, and stress may be released in other directions.

For further analysis, we have sectioned the Coulomb stress field to display cross-sections illustrating the vertical stress field. As shown in Figure 7, there are three cross-sections: A-B, C-D, and E-F. We have oriented these cross-sections so that they are parallel to and perpendicular to the direction of the Palu-Koro Fault.

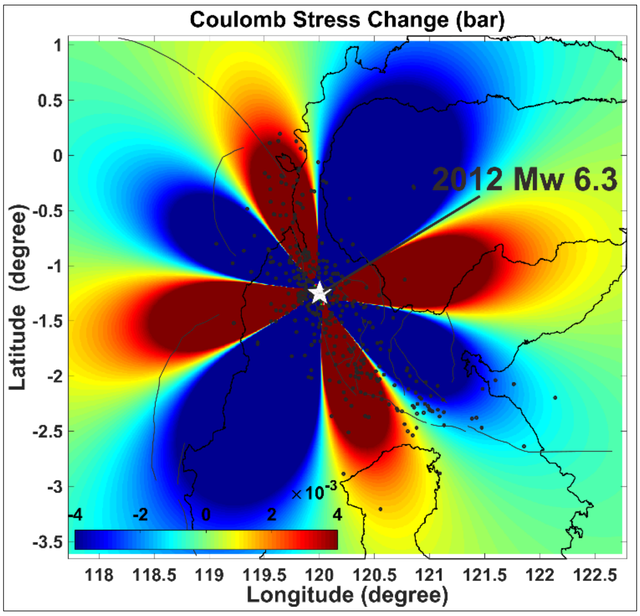

Figure 6. Coulomb stress distribution following the Mw 6.3 earthquake in 2012
Note: Red indicates increasing stress, and blue indicates decreasing stress. The black circular points represent hypocentre locations around the Palu-Koro Fault between 2011 and 2015.

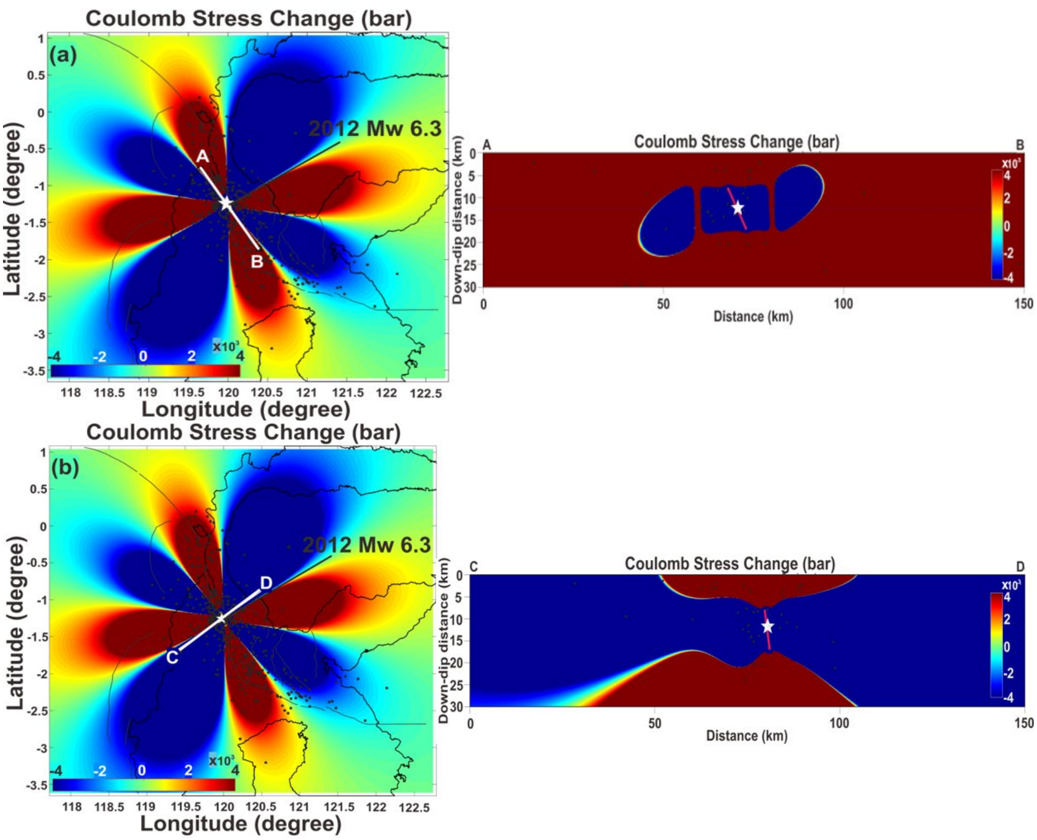

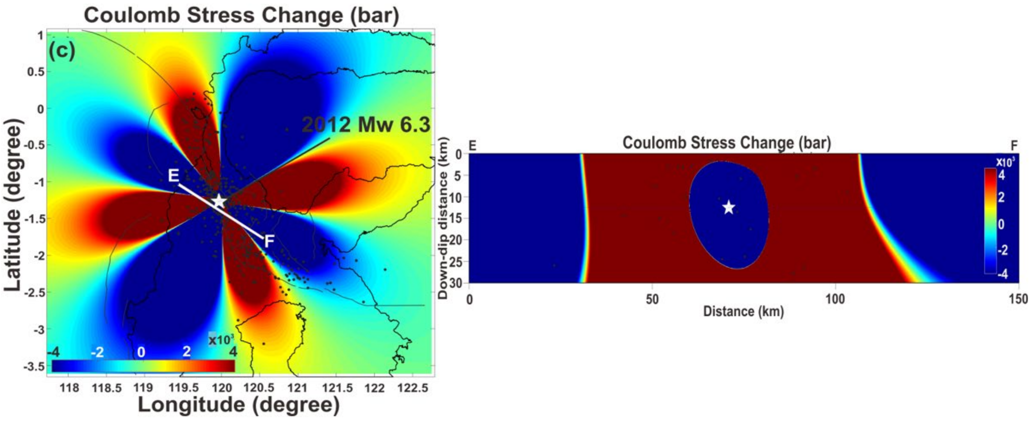

Figure 7. Sections and cross-sections of static Coulomb stress following the 2012 earthquake of magnitude Mw 6.3, down to a depth of 30 km. Section A-B is parallel to the fault plane. Sections C-D and E-F are perpendicular to the fault plane

Note: The black circular points indicate the relocated epicentres of the earthquakes.

4. DISCUSSION

4.1 Hierarchical Density-Based Spatial Clustering of Applications with Noise analysis

HDBSCAN helps better understand areas with high earthquake density. The results show that the area around the epicentre of the 2012 earthquake is the most prominent region in the seismicity distribution. This indicates that the area is significant both as the location of a major earthquake and for consistently exhibiting high seismic activity throughout the analysis period. One of the key strengths of HDBSCAN is its ability to distinguish between large clusters and low-density seismic activity. This distinction is crucial in earthquake analysis. Each earthquake has a different structural significance. Certain events may appear as background activity, whilst others may form part of a consistent active pattern. HDBSCAN separates dense clusters from background noise.

Based on the HDBSCAN map (Figure 4), the concentration of high values around the Palu-Koro Fault zone indicates that this major fault structure controls seismic activity. This is consistent with the fact that the Palu-Koro Fault is one of the most active left-lateral strike-slip faults in Indonesia. Recent integrated studies of gravity, GNSS, and seismic data also show that the Palu-Koro is a highly active left-lateral strike-slip fault and plays a key role in the tectonic framework of Central Sulawesi [27]. Consequently, the earthquake density analysed by HDBSCAN can be linked to crustal deformation processes occurring throughout this fault system.

Furthermore, seismic activity is not concentrated in a single location, as demonstrated by the HDBSCAN clustering results (Figure 5). These areas are scattered along the fault, with some extending southwards. This pattern may indicate a relationship between the main segment of the Palu-Koro Fault and local structures in Central Sulawesi. In the context of earthquake hazard, this information is important, as areas with high seismicity can be prioritised for more detailed seismic monitoring.

4.2 Coulomb stress analysis

Coulomb stress analysis provides a mechanical explanation for the seismicity patterns in the study area. In this study, many hypocentres are located near zones of positive Coulomb stress. This suggests that the stress changes caused by the mainshock, as interpreted, contribute to the distribution of earthquakes following the mainshock. Areas with a higher tendency for shear failure are known as positive Coulomb stress zones. This mechanical interpretation is further supported by clusters of seismic activity surrounding these areas. In other words, these clusters may be caused by physical stress changes in the Earth's crust as well as the proximity of seismic events to one another. This relationship is crucial for understanding the patterns of seismic activity that persist following a major earthquake.

However, not all clusters need to coincide perfectly with the positive stress lobes. Some earthquake epicentres may appear in the transition zone or near the negative stress zone on the map, or even near negative stress zones on the map, though not significantly so. This is likely due to a lack of rupture in those areas, causing them to experience a stress shadow. Given the uncertainty of the Coulomb stress model, this is indeed to be expected. Parameters such as fault plane orientation, the effective friction coefficient, source depth, and assumptions about the medium's elasticity significantly influence earthquake stress values. It has been demonstrated that the distribution of receiving fault planes, as well as spatiotemporal heterogeneity, can affect the results of Coulomb stress analysis [38].

For further analysis, we have divided the Coulomb stress field into several sections to present cross-sections illustrating the vertical stress distribution. As shown in Figure 7, we have used three cross-sections: A-B, C-D, and E-F. Cross-section A-B, which is parallel to the fault plane, and cross-section C-D, which is perpendicular to the fault plane, respectively show a dominant increase in stress (red areas) at depths of 0-10 km and 20-30 km, with a decrease in stress (blue areas) separating these two regions at a depth of 10-20 km (Figures 7(a) and (b)). There is also an increase in stress from depths of 0-30 km, as shown by cross-section E-F (northwest to southeast), which is perpendicular to the fault plane (Figure 7(c)). Cross-sections A-B and C-D show that the earthquakes (represented by points) are largely distributed within the areas of increased stress. However, because this earthquake was a strike-slip event, the distribution of earthquakes (presented by points) is generally spread across both the red and blue lobes (E-F).

Therefore, the interpretation of Coulomb stress in this study must be based on probabilistic and mechanistic approaches. These stress maps are not intended to pinpoint the exact location of the next earthquake, but rather to identify areas that are more likely to experience geological activity. In the context of Palu-Koro, the positive lobe area situated close to the main cluster is best described as an area experiencing a strong post-earthquake stress response.

4.3 Integration of Hierarchical Density-Based Spatial Clustering of Applications with Noise and Coulomb stress

This research does not limit itself to spatial mapping or mechanical interpretation in isolation; rather, it combines two methods with distinct epistemological foundations. Coulomb stress reflects the physical response of the Earth's crust to the redistribution of stress caused by earthquakes, whilst HDBSCAN is a data-driven approach that extracts density structures without considering the shape of the distribution. The combination of the two provides a more robust interpretative framework for understanding post-earthquake mechanisms in the Palu-Koro fault system.

The HDBSCAN clustering results indicate that the distribution of hypocentres is inconsistent and tends to form seismic cores localized around the main Palu-Koro segment (Figure 5).

The quantitative distribution of earthquake data points, in both number and percentage, across the positive and negative ΔCFS is shown in Table 3. Note that because cluster 0 shows no clear spatial relationship with the Coulomb stress pattern (Figure 5), the cluster is classified as noise. Consequently, the cluster is not associated with the ΔCFS.

Table 3 demonstrates that hypocentres in Cluster 1 correlate with ΔCFS > 0, while Cluster 3 gives ΔCFS < 0. Cluster 2 is divided into two sections, one with a positive ACF and the other with a negative ΔCFS, in relatively equal numbers. Additionally, Cluster 4 has 44.33% correlated with ΔCFS positive and 30.05% related to ΔCFS negative.

Table 3. Quantitative distribution and percentage of earthquakes in each cluster

Cluster	ΔCFS > 0 (Red)	ΔCFS < 0 (Blue)	Percent (%) ΔCFS > 0 (Red)	Percent (%) ΔCFS < 0 (Blue)
1	5	0	2.46	0
2	15	16	7.39	7.88
3	0	16	0	7.88
4	90	61	44.33	30.05
Total	110	93	54.19	45.81

On the other hand, the Coulomb stress results indicate that the areas with these clusters are largely situated within zones of Coulomb Failure Stress (ΔCFS > 0). This spatial correlation suggests that structural heterogeneity and the transfer of static stress from the mainshock influenced the seismic activity following the Mw 6.3 earthquake [8]. Specifically, cluster 1 represents the dominant seismic concentration around the main fault and shows the strongest spatial correlation with the positive Coulomb stress region.

Each cluster exhibits a different distribution of earthquake occurrences with respect to changes in Coulomb stress (ΔCFS), as shown in Table 3. Overall, 110 earthquakes (54.19%) occurred in regions with higher Coulomb stress, while 93 earthquakes (45.81%) occurred in regions with lower Coulomb stress. This indicates that most earthquakes occur in areas with higher Coulomb stress, suggesting that fault planes are more likely to fail, particularly as Coulomb stress increases [34, 39].

With 151 earthquake events, or about 74.4% of the total, data cluster 4 was the most dominant. A total of 90 events (59.6%) in this cluster occurred in the ΔCFS > 0 region, while 61 events (40.4%) occurred in the ΔCFS < 0 region. The predominance of ΔCFS > 0 within the largest cluster suggests that seismic activity tends to concentrate in areas under increased stress. Previous studies have shown that static stress transfer can control the distribution of aftershocks and shift the location of subsequent earthquakes toward areas with increased Coulomb stress [39].

Nevertheless, the presence of 61 events in cluster 4 and all 16 events in cluster 3 occurring in regions with ΔCFS < 0 indicates that changes in Coulomb stress are not the sole factor controlling seismic activity. Changes in pore-fluid pressure, heterogeneity in the regional stress field, and the complexity of poorly defined fault geometries can still cause earthquakes to occur in areas with ΔCFS < 0. Furthermore, research conducted on the 2011 Tohoku Earthquake shows that increased seismic activity can also occur in areas conventionally considered to be under shadow stress, particularly at locations where fault systems have various orientations [32].

Although there were only five earthquakes, Cluster 1 was entirely located in the region where ΔCFS > 0, whereas Cluster 2 showed an almost balanced distribution between ΔCFS > 0 and negative values. The local stress conditions of each cluster differ, as indicated by their distinct characteristics. Therefore, the clustering results using HDBSCAN reveal various physical conditions that influence cluster formation and the spatial concentration of earthquakes.

Overall, the results in Table 3 show that clusters with the highest number of events are more likely to be associated with ΔCFS > 0, supporting the hypothesis that stress redistribution contributes to the development of seismic activity around the Palu-Koro Fault. In this case, cluster 0 was excluded because it was correlated with noise. However, the proportion of events in the ΔCFS < 0 region remains substantial, indicating that the interpretation of Coulomb stress must be integrated with other geological components. Therefore, a more comprehensive understanding of the spatial patterns of seismicity can be obtained by integrating HDBSCAN and Coulomb stress analysis rather than using the two methods separately.

This study broadens our understanding of the Palu-Koro Fault system, an active fault with complex segmentation. Seismic activity is not only concentrated around the epicenter, but also spreads in various directions along fault lines and structures surrounding the epicenter. This pattern suggests that the stability of several areas surrounding the source of the Mw 6.3 earthquake in 2012 may be compromised. These segments are of great importance for studies on earthquake hazard potential. Segments showing dense seismic clusters together with positive Coulomb stress conditions represent areas where stress loading and earthquake activity occur simultaneously, making them important targets for seismic hazard evaluation, as they are most likely to experience increased seismic activity following a major earthquake. Conversely, segments showing sparser clusters but still following fault structures should be regarded as transition zones or areas of moderate seismic activity.

The integration of probabilistic hypocentre relocation, density-based clustering (HDBSCAN), and Coulomb stress modeling within a single interpretation pipeline is the key strength of this method. This method enables cross-validation between statistical structures (cluster stability) and physical controls (stress transfer). The results not only indicate areas of concentrated earthquake activity but also provide further insight into why such spatial concentrations form.

One of the key benefits of this integration is the ability to identify fault segments that simultaneously exhibit high seismicity density and stress loading. In this study, Clusters 1, 2, and 4 represent conditions in which dense seismicity coincides with positive ΔCFS values. Conversely, clusters located outside the strongest stress-loading regions highlight the influence of additional geological factors beyond static stress transfer.

5. CONCLUSIONS

This study presents an integrated seismic interpretation framework that combines probabilistic hypocentre relocation, HDBSCAN clustering, and Coulomb stress modeling to investigate post-earthquake deformation along the Palu-Koro Fault following the Mw 6.3 earthquake on 18 August 2012. The results indicate that the distribution of earthquakes is influenced by the combined effects of structural segmentation and the redistribution of static stress, rather than by random spatial occurrence.

The HDBSCAN algorithm effectively identifies stable, high-density seismic nuclei and separates diffuse background seismic activity without imposing a predefined cluster structure. These seismic nuclei represent physically meaningful concentrations of earthquake activity along fault systems. Further Coulomb stress modeling showed that the majority of these clusters are spatially associated with positive Coulomb failure stress anomalies, indicating an increased potential for failure due to co-seismic stress transfer.

The main result of this study is the identification of stress-consistent seismic cores, defined as clustered concentrations of hypocentres coinciding with regions of stress loading. These findings establish a mechanical link between statistical seismicity patterns and geophysical stress evolution, thereby enabling earthquake clusters to be interpreted not only as spatial groupings but also as indicators of mechanically critical fault segments.

ACKNOWLEDGMENT

This research is funded by Institut Teknologi Sepuluh Nopember (ITS) Surabaya and managed under the Strategic Research Grant (SRG) Type C Scheme (Contract No. 1432/PKS/ITS/2026). We are grateful to the Meteorological, Climatological, and Geophysical Agency (BMKG) for making catalogue data available. HJ was awarded the BPPDN 2019 Scholarship from the Ministry of Research, Technology, and Higher Education of the Republic of Indonesia for this research.

REFERENCES

[1] Bellier, O., Sébrier, M., Seward, D., Beaudouin, T., Villeneuve, M., Putranto, E. (2006). Fission track and fault kinematics analyses for new insight into the late Cenozoic tectonic regime changes in West-Central Sulawesi (Indonesia). Tectonophysics, 413(3-4): 201-220. https://doi.org/10.1016/j.tecto.2005.10.036

[2] Watkinson, I.M., Hall, R. (2017). Fault systems of the eastern Indonesian triple junction: Evaluation of Quaternary activity and implications for seismic hazards. Geological Society, London, Special Publications, 441(1): 71-120. https://doi.org/10.1144/SP441.8

[3] Lee, S.J., Wong, T.P., Lin, T.C., Liu, T.Y. (2019). Complex triggering supershear rupture of the 2018 M W 7.5 Palu, Indonesia, earthquake determined from teleseismic source inversion. Seismological Research Letters, 90(6): 2111-2120. https://doi.org/10.1785/0220190111

[4] Bellier, O., Sébrier, M., Beaudouin, T., et al. (2001). High slip rate for a low seismicity along the Palu-Koro active fault in central Sulawesi (Indonesia). Terra Nova, 13(6): 463-470. https://doi.org/10.1046/j.1365-3121.2001.00382.x

[5] Socquet, A., Simons, W., Vigny, C., et al. (2006). Microblock rotations and fault coupling in SE Asia triple junction (Sulawesi, Indonesia) from GPS and earthquake slip vector data. Journal of Geophysical Research: Solid Earth, 111(B8): B08409. https://doi.org/10.1029/2005JB003963

[6] Sipayung, R., Ulfiana, E., Sianipar, D. (2018). The connection of Coloumb stresses and aftershock imparted by the 18 August 2012 Mw 6.3 Palu-Koro earthquake. AIP Conference Proceedings, 1987(1): 020037. https://doi.org/10.1063/1.5047322

[7] Khairina, F., Chen, W., Wei, S., Suardi, I. (2017). Focal mechanism of the August 18th 2012 Mw6. 3 Palu-Koro earthquake and its implication of seismic hazard. AIP Conference Proceedings, 1857(1): 050003. https://doi.org/10.1063/1.4987081

[8] Liu, C., Shi, Y. (2022). The role of fault interaction in earthquake migration in Central Sulawesi, Indonesia. Tectonophysics, 839: 229530. https://doi.org/10.1016/j.tecto.2022.229530

[9] Stein, R.S. (1999). The role of stress transfer in earthquake occurrence. Nature, 402(6762): 605-609. https://doi.org/10.1038/45144

[10] Jayadi, H., Musa, M.D.T., Rachman, G., Meidji, I.U., Massinai, M.F.I., Warnana, D.D. (2025). A non-linear hypocenter localization along the active Palu-Koro fault: A case study Central Sulawesi. Indonesian Physical Review, 8(2): 400-416. https://doi.org/10.29303/ipr.v8i2.418

[11] Lomax, A., Virieux, J., Volant, P., Berge-Thierry, C. (2000). Probabilistic earthquake location in 3D and layered models: Introduction of a Metropolis-Gibbs method and comparison with linear locations. In Advances in Seismic Event Location, pp. 101-134. https://doi.org/10.1007/978-94-015-9536-0_5

[12] Lomax, A., Savvaidis, A. (2022). High-precision earthquake location using source-specific station terms and inter-event waveform similarity. Journal of Geophysical Research: Solid Earth, 127(1): 1-28. https://doi.org/10.1029/2021JB023190

[13] Rachman, G., Santosa, B.J., Rohadi, S., Nugraha, A.D., Rosalia, S. (2021). Preliminary results: Probabilistic non-linear method to determine the hypocenter location in the Molucca Sea collision zone from BMKG networks. IOP Conference Series: Earth and Environmental Science, 873(1): 012026. https://doi.org/10.1088/1755-1315/873/1/012026

[14] Fan, Z., Xu, X. (2019). Application and visualization of

typical clustering algorithms in seismic data analysis. Procedia Computer Science, 151: 171-178. https://doi.org/10.1016/j.procs.2019.04.026
[15] Cesca, S. (2020). Seiscloud, a tool for density-based seismicity clustering and visualization. Journal of Seismology, 24(3): 443-457. https://doi.org/10.1007/s10950-020-09921-8
[16] Scarfì, L., Barreca, G., Cassisi, C., Langer, H. (2025). Earthquake clustering and structural modelling unravel volcano-tectonic complexity beneath Mount Etna. Scientific Reports, 15(1): 18607. https://doi.org/10.1038/s41598-025-03321-z
[17] Kurniawati, I., Adhi, M.A., Arriza, H.H., Sinambela, M. (2025). Comparative clustering of earthquake data in Central Java using DBSCAN, HDBSCAN, STDBSCAN, and Fuzzy C-Means. In 2025 5th International Conference on Electronic and Electrical Engineering and Intelligent System (ICE3IS), Yogyakarya, Indonesia, pp. 508-513. https://doi.org/10.1109/ICE3IS66769.2025.11280729
[18] Rahman, M.F., Liu, W., Suhaim, S.B., Thirumuruganathan, S., Zhang, N., Das, G. (2016). HDBSCAN: Density based clustering over location based services. arXiv preprint arXiv:1602.03730. https://doi.org/10.48550/arXiv.1602.03730
[19] Tran, T.H., Cao, T.D., Tran, T.T.H. (2021). HDBSCAN: Evaluating the performance of hierarchical clustering for big data. In Soft Computing: Biomedical and Related Applications, pp. 273-283. https://doi.org/10.1007/978-3-030-76620-7_24
[20] Dewanto, B.G., Wijaya, C., Priadi, R. (2025). The Palu-Koro fault behaviour monitoring associated with the 2018 Palu earthquake based on the multi-temporal PlanetScope and Landsat 8 satellite images. Remote Sensing Applications: Society and Environment, 37: 101397. https://doi.org/10.1016/j.rsase.2024.101397
[21] Natawidjaja, D.H., Daryono, M.R., Prasetya, G., et al. (2021). The 2018 M w7. 5 Palu 'supershear' earthquake ruptures geological fault's multisegment separated by large bends: Results from integrating field measurements, LiDAR, swath bathymetry and seismic-reflection data. Geophysical Journal International, 224(2): 985-1002. https://doi.org/10.1093/gji/ggaa498
[22] Jalil, A., Fathani, T.F., Satyarno, I., Wilopo, W. (2021). Liquefaction in Palu: The cause of massive mudflows. Geoenvironmental Disasters, 8(1): 21. https://doi.org/10.1186/s40677-021-00194-y
[23] Hall, R.A., Wilson, M.E.J. (2000). Neogene sutures in eastern Indonesia. Journal of Asian Earth Sciences, 18(6): 781-808. https://doi.org/10.1016/S1367-9120(00)00040-7
[24] van Leeuwen, T., Allen, C.M., Elburg, M., Massonne, H.J., Palin, J.M., Hennig, J. (2016). The Palu metamorphic complex, NW Sulawesi, Indonesia: Origin and evolution of a young metamorphic terrane with links to Gondwana and Sundaland. Journal of Asian Earth Sciences, 115: 133-152. https://doi.org/10.1016/j.jseaes.2015.09.025
[25] Patria, A., Putra, P.S. (2020). Development of the Palu–Koro fault in NW Palu valley, Indonesia. Geoscience Letters, 7(1): 1-11. https://doi.org/10.1186/s40562-020-0150-2
[26] Kusumawati, D., Sahara, D.P., Puspito, N.T., et al. (2024). A new moment tensor catalogue of light to moderate earthquakes in Palu-Koro and Matano faults, Sulawesi, based on the regional network in Indonesia: Fault analysis and insight. Physics of the Earth and Planetary Interiors, 352: 107209. https://doi.org/10.1016/j.pepi.2024.107209
[27] Heliani, L.S., Pratama, C., Anggraini, A., Dewanto, B.G., Natul, A.S., Lestari, D. (2025). Integrated gravity, GNSS, and seismic analysis for fault mapping in Sulawesi Island: Insights into the Palu-Koro Fault. Geodesy and Geodynamics, 17(3): 326-340. https://doi.org/10.1016/j.geog.2025.07.001
[28] Jaya, A., Nishikawa, O., Jumadil, S. (2019). Distribution and morphology of the surface ruptures of the 2018 Donggala–Palu earthquake, Central Sulawesi, Indonesia. Earth, Planets and Space, 71(1): 144. https://doi.org/10.1186/s40623-019-1126-3
[29] Geological Map of Indonesia, Ujung Pandang Sheet. Geological Research and Development Centre, Indonesia. https://geologi.esdm.go.id/geomap/pages/preview/peta-geologi-indonesia-lembar-ujung-pandang.
[30] Wells, D.L., Coppersmith, K.J. (1994). New empirical relationships among magnitude, rupture length, rupture width, rupture area, and surface displacement. Bulletin of the Seismological Society of America, 84(4): 974-1002. https://doi.org/10.1785/BSSA0840040974
[31] Lin, J., Stein, R.S. (2004). Stress triggering in thrust and subduction earthquakes and stress interaction between the southern San Andreas and nearby thrust and strike-slip faults. Journal of Geophysical Research: Solid Earth, 109(B2). https://doi.org/10.1029/2003JB002607
[32] Toda, S., Stein, R.S., Richards-Dinger, K., Bozkurt, S.B. (2005). Forecasting the evolution of seismicity in southern California: Animations built on earthquake stress transfer. Journal of Geophysical Research: Solid Earth, 110(B5). https://doi.org/10.1029/2004JB003415
[33] Strobl, M., Sander, J., Campello, R.J.G.B., Zaïane, O. (2020). Model-based clustering with HDBSCAN. In Joint European Conference on Machine Learning and Knowledge Discovery in Databases, pp. 364-379. https://doi.org/10.1007/978-3-030-67661-2_22
[34] King, G.C.P., Stein, R.S., Lin, J. (1994). Static stress changes and the triggering of earthquakes. Bulletin of the Seismological Society of America, 84(3): 935-953. https://doi.org/10.1785/BSSA0840030935
[35] Supendi, P., Nugraha, A.D., Widiyantoro, S., et al. (2020). Relocated aftershocks and background seismicity in eastern Indonesia shed light on the 2018 Lombok and Palu earthquake sequences. Geophysical Journal International, 221(3): 1845-1855. https://doi.org/10.1093/gji/ggaa118
[36] Jia, Y., He, T., Wang, L. (2025). Trajectory clustering based on FB-HDBSCAN algorithm. Journal of Physics: Conference Series, 3078(1): 012050. https://doi.org/10.1088/1742-6596/3078/1/012050
[37] Wang, S.M., Yang, W.R., Zhuang, Q.Y., et al. (2025). Application of three-dimensional hierarchical density-based spatial clustering of applications with noise in ship automatic identification system trajectory-cluster analysis. Applied Sciences, 15(5): 2621. https://doi.org/10.3390/app15052621
[38] Ishibe, T., Ogata, Y., Tsuruoka, H., Satake, K. (2017). Testing the Coulomb stress triggering hypothesis for three recent megathrust earthquakes. Geoscience Letters,

4(1): 5. https://doi.org/10.1186/s40562-017-0070-y
[39] Stein, R.S., King, G.C.P., Lin, J. (1994). Stress triggering of the 1994 M = 6.7 Northridge, California, earthquake by its predecessors. Science, 265(5177): 1432-1435. https://doi.org/10.1126/science.265.5177.1432